Electromagnetic Interference (EMI) Shielding of Single-Walled Carbon Nanotube Epoxy Composites

Ning Li,[†] Yi Huang,[†] Feng Du,[†] Xiaobo He,[‡] Xiao Lin,[‡] Hongjun Gao,[‡] Yanfeng Ma,[†] Feifei Li,[†] Yongsheng Chen,*,[†] and Peter C. Eklund*,[§]

Key Laboratory of Functional Polymer Materials and Center for Nanoscale Science and Technology, Institute of Polymer Chemistry, College of Chemistry, Nankai University, Tianjin, 300071, China, The Institute of Physics, Chinese Academy of Sciences, Beijing 100080, China, and Departments of Physics and Materials Science and Engineering, The Pennsylvania State University, University Park, Pennsylvania 16802-6300

ABSTRACT

Single-walled carbon nanotube (SWNT)−polymer composites have been fabricated to evaluate the electromagnetic interference (EMI) shielding effectiveness (SE) of SWNTs. Our results indicate that SWNTs can be used as effective lightweight EMI shielding materials. Composites with greater than 20 dB shielding efficiency were obtained easily. EMI SE was tested in the frequency range of 10 MHz to 1.5 GHz, and the highest EMI shielding efficiency (SE) was obtained for 15 wt % SWNT, reaching 49 dB at 10 MHz and exhibiting 15−20 dB in the 500 MHz to 1.5 GHz range. The EMI SE was found to correlate with the dc conductivity, and this frequency range is found to be dominated by reflection. The effects of SWNT wall defects and aspect ratio on the EMI SE were also studied.

Because of their unique structure and properties, single-walled and multiwalled carbon nanotubes (SWNTs and MWNTs) have been investigated for many potential applications.[1,2] Particularly, their fascinating electrical and mechanical properties offer a new arena for the development of advanced engineering materials.[3−7] Electromagnetic interference (EMI) shielding of radio frequency radiation continues to be a serious concern in society. Lightweight EMI shielding is needed to protect the workspace and environment from radiation coming from computers and telecommunication equipment as well as for protection for sensitive circuits. Compared to conventional metal-based EMI shielding materials, electrically conducting polymer composites have gained popularity recently because of their light weight, resistance to corrosion, flexibility, and processing advantages.[8−15]

The EMI shielding efficiency (SE) of a composite material depends on many factors, including the filler's intrinsic conductivity, dielectric constant, and aspect ratio.[8,10] The small diameter, high aspect ratio, high conductivity, and mechanical strength of carbon nanotubes (CNTs), including

SWNTs and MWNTs, make them an excellent option for creating conductive composites for high-performance EMI shielding materials at low filling. For example, MWNTs have been added to polymer matrixes for EMI shielding materials and tested in the frequency range of 8.2−12.4 GHz (X band) with 20 dB for 7% MWNTs loading in polystyrene (PS).[16,17] Joo et al. studied the electrical conductivity and EMI properties of MWNTs in poly(methyl methacrylate) (PMMA) containing Fe. They achieved 27 dB for 40% MWNTs loading.[18] MWNT composites with encapsulated Fe have also been studied for their microwave absorption, but with a different phases and shapes of included Fe.[19] Very recently, Xiang et al. synthesized MWNT composites with silica and studied their microwave attenuation in the X band.[12] Earlier, Grimes et al.[20] reported that SWNT−polymer composites possess high real permittivity (polarization, ϵ') as well as imaginary permittivity (adsorption or electric loss, ϵ'') in the 0.5−2 GHz range. They found that the permittivity decreases rapidly with increasing frequency. Recent studies have reported that SWNTs can be dispersed into epoxy with a very low percolation threshold.[9,21,22]

In this work, we report the first results of EMI shielding studies of nanotube−polymer composites based on SWNTs. Our results indicate that our composites can provide effective shielding for mobile phone systems that operate near ∼1 GHz.[23] All previous EMI studies on nanotube−polymer

---

* To whom correspondence should be addressed. Tel: + 86 (22) 2350-0693. Fax: + 86 (22) 2350-2749. E-mail: yschen99@nankai.edu.cn; pce3@psu.edu.
† Nankai University. N. Li and Y. Huang contributed equally to this work.
‡ Chinese Academy of Sciences.
§ The Pennsylvania State University.

composites have been carried out with MWNTs.[12,16−19] The electrical properties of small-diameter SWNTs are distinctly different from their larger-diameter MWNT counterparts. Small-diameter (i.e., $1 < d < 2$ nm) SWNTs can be either metallic or semiconducting depending on their chirality integers (n,m). The energy band gaps of these tubes are in the range of $0.5−1$ eV, that is, the gaps are large compared to kT and, in the absence of defects, the thermally produced free carrier concentrations should be low near room temperature. In addition, small-diameter metallic SWNTs have been found to be exceptional metals, even exhibiting ballistic transport at low temperature.[24,25] MWNTs, however, because of the larger inherent diameter of SWNTs present in the concentric tube shells (i.e., $d > 5$ nm), should be approximately zero gap semiconductors or exhibit very weak band overlap, leading to weak semi-metallic behavior. Thus, per unit wt % added to the polymer host, the nature of the EMI shielding properties of MWNT− and SWNT−polymer composites are expected to be altogether different.

To produce SWNT−polymer composites for EMI shielding, we have formed well-dispersed SWNT−epoxy resin composites using an in situ process described below. SWNTs used in this work were made with a modified arc-discharge apparatus using Ni/Y as the catalyst.[26,27] Because it is well known that the filler's particle size and length/diameter aspect ratio have a significant impact on the composite's percolation point and its EMI performance, we have studied SWNTs with different aspect ratios and/or wall structures for the composite fabrication. They were obtained as follows: (1) arc vaporization using He as the carrier gas in the arc chamber; this material exhibited the largest bundle length/diameter aspect ratio (i.e., referred to here as "SWNTs-long"); (2) arc vaporization using He/10% CO_2 as the carrier gas; these materials exhibit smaller aspect ratio (referred to here as "SWNTs-short"); and (3) material obtained after annealing "SWNTs-short" at 1100 °C for 3 h in a tube furnace under N_2 (referred to here as "SWNTs-annealed"); these tube bundles exhibit enhanced conductivity due to the removal of wall defects and functional groups.

A commercially available bisphenol A-type epoxy resin (618 type, Tianjin Resin Company) and an amine-type hardener ($[C_{17}H_{31}CONH(C_2H_4NH)_2H]_2$, Tianjin Ningping Chemical Co., LTD, Model: A022-2) were used to prepare the polymer matrix. The resin/curing agent ratio was 2/1. Briefly, SWNTs were first dispersed in acetone in an ultrasonic bath (Gongyi Yuhua Instrument Co., LTD, Model: KQ400B, 400 W) at room temperature for 2 h and then an epoxy resin/acetone solution was added to the suspension of SWNTs. After the mixture was again sonicated for 2 h, the hardener was added during mechanical stirring. The mixture was further sonicated for 15 min, and then the mixture was poured into suitable molds to allow the acetone to evaporate completely. The composite was cured further at room temperature overnight.

The dc electrical conductivity of the SWNTs/epoxy composites was determined using the standard four-point contact method on rectangular sample slabs in order to eliminate contact-resistance effects. Data were collected with
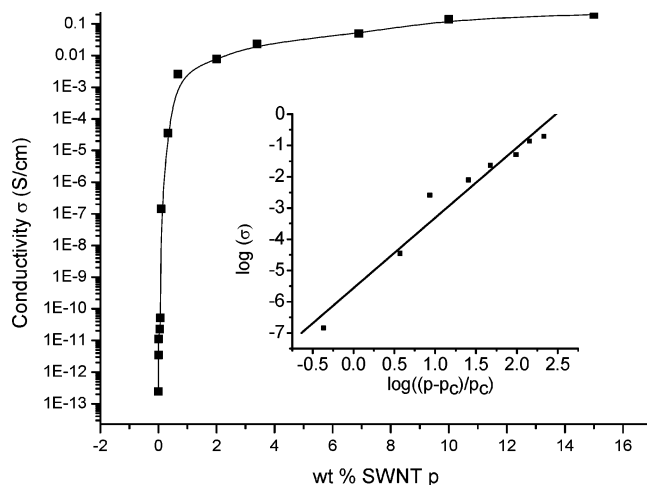

Figure 1. log DC conductivity (σ) vs mass fraction (p) of SWNTs-long composites measured at room temperature. Inset: log−log plot for σ vs $((p − p_c)/p_c)$ for the same composites. The straight line in the inset is a least-squares fit to the data using eq 1 returning the best fit values $p_c = 0.062\%$ and $\beta = 2.68$.

a Keithley SCS 4200. Figure 1 shows the dc conductivity (σ) of SWNTs/epoxy composites as a function of SWNTs mass fraction (p). As can be seen, below 0.6 wt %, the conductivity displays a dramatic increase of 10 orders of magnitude, indicating the formation of percolating network. The inset in Figure 1 shows that the electrical conductivity obeys the power law[28]

$$\sigma \propto (\nu − \nu_c)^{\beta} \qquad (1)$$

where σ is the composite conductivity, ν is the SWNT volume fraction, ν_c is the percolation threshold, and β is the critical exponent. Because the densities of the polymer and the SWNT are similar, we assume that the mass fraction, p, and volume fraction, ν, of the SWNTs in the polymer are almost the same. As shown in the inset of Figure 1 for the $\log(\sigma)$ versus $\log((p − p_c)/p_c)$ plot, the SWNT/epoxy composite conductivity agrees very well with the percolation behavior predicted by eq 1. As can be seen, the straight line in the figure with $p_c = 0.062\%$ and $\beta = 2.68$ gives an excellent fit to the data with a correlation factor of 0.98. The percolation threshold is found to be quite low, that is, 0.062 wt % SWNT, indicating a very efficient dispersion of SWNTs into the polymer matrix at low concentration. The value of the critical exponent, β, is found to be in good agreement with the theoretical results for a percolating rod network system.[9,29] Our values for the percolation thresholds in our polymer−epoxy materials are in good agreement with studies by Kim et al.[21] for their SWNTs−epoxy system.

Figure 2 shows a representative SEM image (Hitachi S-3500N) for the cross section of the 10 wt % SWNT loading composite. The image shows that the SWNTs were dispersed homogeneously within the epoxy matrix. Apart from the very low percolation threshold, we also observed that the conductivity reaches 0.20 S/cm at 15 wt % SWNT loading. This value is 12 orders of magnitude higher than that of the pure epoxy resin (i.e., $2.44 \times 10^{−13}$ S/cm).
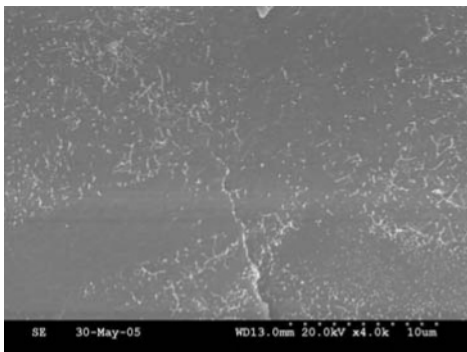
Figure 2. SEM image of the cross section of SWNTs-long/epoxy composites with 10 wt % loading.
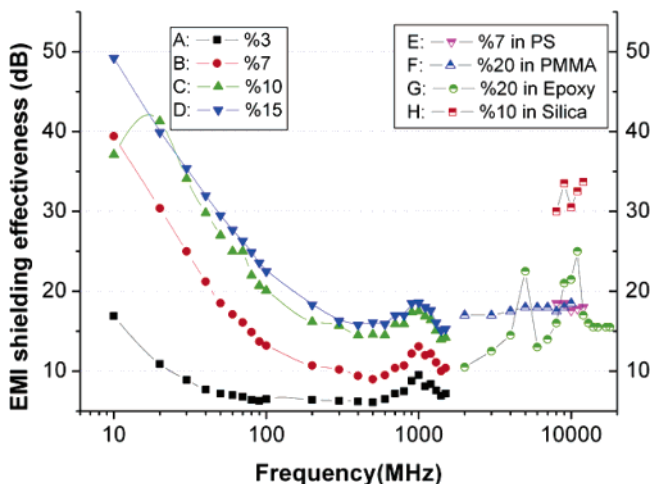
Figure 3. EMI shielding effectiveness (plots labeled A−D) for SWNT−polymer materials (wt % 3−15) studied in this work (10 MHz to 1.5 GHz). Plots labeled E−H are higher frequency data on MWNT-based material presented for comparison: E, MWNTs in PS from ref 16; F, MWNTs in PMMA from ref 18; G, MWNTs in epoxy resin from ref 19 and the value of the y axis for G is the reflection loss; H, MWNTs in silica from ref 12.

It is well established that the EMI shielding effectiveness of a conductive composite is strongly related to its dc conductivity. The EMI shielding effectiveness (SE) of a material is defined as $SE(dB) = -10 \log(P_t/P_0)$, where P_t and P_0 are, respectively, the transmitted and incident electromagnetic power. For example, an attenuation of the incident beam by a factor of 100 (i.e., 1% transmission) is equivalent to 20 decibels (dB) of attenuation. In this study, the EMI shielding effectiveness of SWNT−epoxy composites was measured with a HP8753C vector network analyzer using an industrial standard method. Composite slabs of dimensions $180 \times 180 \times 1.5$ mm were measured in the 10 MHz − 1.5 GHz frequency range. Figure 3 shows the variation of the EMI shielding effectiveness over the frequency range of 10 MHz − 1.5 GHz for various SWNT loadings. It is observed that at fixed frequency SE increases with increasing wt % of SWNTs. For a fixed SWNT wt %, SE increases with decreasing frequency in our measured frequency range. The highest SE we observed was for the composite with 15 wt % SWNTs-long, that is, $SE = 49.2$ dB at 10 MHz. At higher frequencies, the composites made from SWNTs-long exhibited $SE \approx 20$ dB at ∼1 GHz for

both the 10 and 15 wt % loadings. The target value of the EMI shielding effectiveness needed for commercial applications is around 20 dB (i.e., equal to or less than 1% transmission of the electromagnetic wave). Thus, our results indicate that SWNT/epoxy composites with 10−15 wt % loadings can meet the commercial application SE demands and can be useful, for example, in mobile cell applications.

When electromagnetic radiation is incident on a slab of material, the absorptivity (A), reflectivity (R), and transmissivity (T) must sum to the value "one", that is, $T + R + A = 1$. The total EMI shielding effectiveness (SE_{total}) is the sum of contributions from absorption (SE_A), reflectance (SE_R), and multiple reflection (SE_M), for example, $SE_{total} = SE_A + SE_R + SE_M$. When $SE_{total} > 15$ dB, it is usually assumed that $SE_{total} \approx SE_A + SE_R$ (i.e., SE_M is negligible). Using the equations $SE_R = -10 \log R$, $SE_{total} = -10 \log T$ and $A = 1 - T - R$, we can therefore get absorptivity (A), reflectivity (R), and transmissivity (T). In this work, for the SWNTs-long epoxy composite with 10 wt % loading, the reflectivity (R), absorptivity (A), and transmissivity (T) are 0.90, 0.08, and 0.02 at 1.0 GHz. Thus, the contribution of reflection to the total EMI shielding effectiveness is much larger than that from absorption. Similar results were observed at other frequencies and with other loadings above the percolation threshold. Similar findings were reported in the investigation of the shielding mechanism of MWNT polystyrene composites.[16,17] For the PMMA−MWNTs with Fe[18] and epxoy−MWNTs with crystalline Fe,[19] it was observed that the contribution from absorption to total EMI SE was larger than that from reflection. However, the authors identified this with the ferromagnetic Fe in the system.

In Figure 3, for comparison to our SWNT EMI shielding results at four wt % loadings, we also display data for the most significant MWNT composite results in the literature.[12,16,18,19] These MWNT studies were made in the frequency range of 2−20 GHz (X-band), that is, a decade higher frequencies than the present studies. As can be seen in the figure, the composites of MWNTs based on silica,[12] (polystyrene) PS,[16] and PMMA[18] exhibit a nearly frequency-independent EMI SE performance. For the MWNT−epoxy composite with additional crystalline needle-shaped α-Fe,[19] the reflection loss was found to fluctuate with frequency and identified with the inclusion of Fe. In agreement with our results, all of these studies found that the contribution to the EMI SE from reflection is much larger than that from absorption,[12,16,17] except when high mass density ferromagnetic Fe is in the system.[18,19] Compared with our measured SWNT bundle percolation threshold 0.06% (SWNTs-long), a higher percolation threshold of 0.3% was observed for the MWNT composites with PMMA.[18]

There have been many intensive studies to learn how to achieve low wt % percolation thresholds for various MWNT[12,17,18,30−34] and SWNT[9,20,35−38] composites. In some cases, the results were found to outperform current technologies based on other additives. Even though one might anticipate that wall defects and the aspect ratio are important parameters affecting the EMI SE, their impact on EMI shielding has not yet been explored in MWNT−polymer
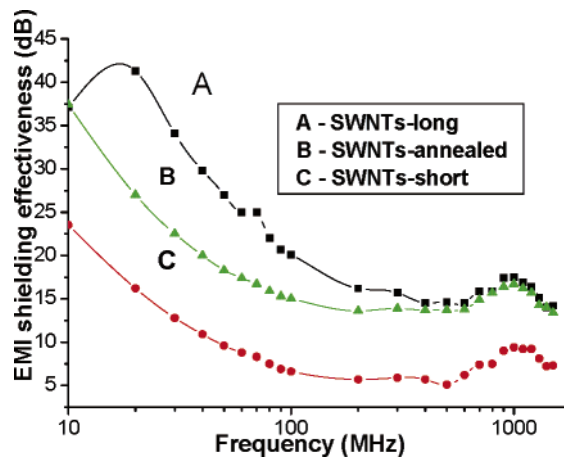
Figure 4. Impact of wall integrity and aspect ratio on the EMI shielding effectiveness of the composites containing 10 wt % SWNTs.

composites.[23] Indeed, according to percolation theory, if the conductive filler in the matrix has a high aspect ratio, then the filler forms a conductive network at lower wt %. For example, Yodh et al. reported detailed dc conductivity studies for composites with different SWNTs, and they found that the SWNT bundle aspect ratio significantly impacts the threshold concentration and the composites' conductivity.[9] Once percolation is achieved, the EM theory indicates that the EMI SE increases dramatically.[10] Thus, for all of these reasons, we were therefore motivated to study how the SWNT aspect ratio and its surface structure/morphology affect the SWNT−epoxy EMI performance. The results of our studies are presented below.

Figure 4 shows our EMI SE data for three of our composites containing 10 wt % of SWNTs, that is, composites with identical polymer, but based on "SWNTs-long", "SWNTs-short", and "SWNTs-annealed", as defined above. For the same wt % loading, it is observed that the shielding effectiveness of SWNTs-short composite is much lower than that of SWNTs-long composite. This is consistent with EM theory and the measured dc conductivities (0.05 S/cm, SWNTs-short; and 0.14 S/cm, SWNTs-long). The SWNT-annealed composites (based on annealed SWNTs-short material) were found to exhibit a significant increase in EMI SE over that observed for the same SWNT wt % composites made from SWNTs-short. In our previous work,[27] using AFM, we have found that the average aspect ratio of bundles of SWNTs-short ($L/D = 740/5.32 = 139$, $\pm 8\%$ error) is significantly lower than that ($1430/5.95 = 240$) of SWNTs-long. Figure 5 presents typical AFM statistics demonstrating the effect of arc growth conditions on the distributions for SWNT bundle length and diameter. It can be seen that SWNTs-short generated using He/10%CO_2 as the carrier gas are significantly shorter than SWNTs-long generated using He. From the simplified percolation and EMI theories for the isotropic dispersion of a random rod network,[9] the SWNT composites with higher SWNT bundle aspect ratios are predicted to have lower percolation threshold concentrations, higher conductivities, and better EMI shielding performances under the same wt % loading. Indeed, the composite with
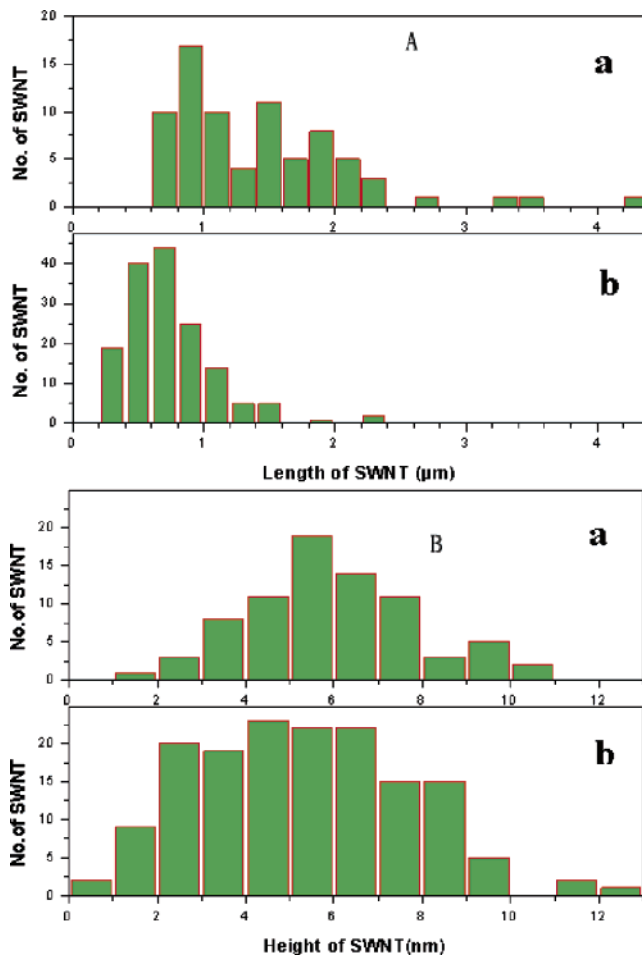
Figure 5. Effect of arc growth conditions on SWNT bundle diameter and length, as measured by AFM; length (A) and height (B). SWNTs prepared under (a) pure He buffer gas and (b) 10 vol % CO_2/He buffer gas. The average length of SWNTs is 1.43 and 0.74 μm for pure He and 10% CO_2/He buffer gas. The average diameter of a SWNT bundle is 5.95 and 5.32 nm, respectively, for pure He and 10% CO_2/He buffer gas. Error was estimated to be ∼8%. For AFM characterization, all samples (1 mg) were sonicated in DMF (100 mL) for 2 h.

SWNTs-long is observed to exhibit better EMI SE, as shown in Figure 4.

It is well known that high-temperature annealing of SWNTs in inert gas or vacuum can remove wall defects. This annealing treatment is therefore expected to improve the dc conductivity and thus the EMI SE. We observed these effects, as can be seen in Figure 4. It is worth noting that although the EMI shielding effectiveness increases significantly after high-T annealing, these composites still exhibited lower EMI SE than composites of the same loading based on SWNTs-long. This observed SE is also consistent with the observed conductivities (0.14 S/cm vs 0.12 S/cm). On the basis of all of these results, we can conclude that a high aspect ratio of the SWNT bundles in SWNT−epoxy composites is the most important parameter for improving EMI SE.

In summary, the EMI SE and conductivity of SWNT−epoxy composites based on SWNTs with different aspect ratios and wall defects have been studied. The highest EMI

shielding effectiveness for SWNT−epoxy composites was found for materials with 15 wt % SWNTs-long as the additive. The SE is found to be ∼49 dB at 10 MHz, and the shielding effectiveness is around 15−20 dB in the 500 MHz to 1.5 GHz range. These results indicate that SWNT−polymer composites could be used as an effective and lightweight EMI shielding material. We also observed a strong correlation between the EMI SE and the dc conductivity, in agreement with the EMI shielding theory. The EMI shielding SE was found to be dominated by reflection. We also demonstrated that SWNT−polymer composites with higher SWNT bundle aspect ratios and better nanotube wall integrities enhance the EMI performance significantly.

References

(1) Iijima, S.; Ichihashi, T. *Nature* **1993**, *363*, 603.
(2) Baughman, R. H.; Zakhidov, A. A.; de Heer, W. A. *Science* **2002**, *297*, 787.
(3) Baughman, R. H.; Cui, C. X.; Zakhidov, A. A.; Iqbal, Z.; Barisci, J. N.; Spinks, G. M.; Wallace, G. G.; Mazzoldi, A.; De Rossi, D.; Rinzler, A. G.; Jaschinski, O.; Roth, S.; Kertesz, M. *Science* **1999**, *284*, 1340.
(4) Minoux, E.; Groening, O.; Teo, K. B. K.; Dalal, S. H.; Gangloff, L.; Schnell, J. P.; Hudanski, L.; Bu, I. Y. Y.; Vincent, P.; Legagneux, P.; Amaratunga, G. A. J.; Milne, W. I. *Nano Lett.* **2005**, *5*, 2135.
(5) Semet, V.; Binh, V. T.; Guillot, D.; Teo, K. B. K.; Chhowalla, M.; Amaratunga, G. A. J.; Milne, W. I.; Legagneux, P.; Pribat, D. *Appl. Phys. Lett.* **2005**, *87*, 223103.
(6) Zhang, M.; Fang, S. L.; Zakhidov, A. A.; Lee, S. B.; Aliev, A. E.; Williams, C. D.; Atkinson, K. R.; Baughman, R. H. *Science* **2005**, *309*, 1215.
(7) Dresselhaus, M. S. *Nature* **2004**, *432*, 959.
(8) Joo, J.; Lee, C. Y. *J. Appl. Phys.* **2000**, *88*, 513.
(9) Bryning, M. B.; Islam, M. F.; Kikkawa, J. M.; Yodh, A. G. *Adv. Mater.* **2005**, *17*, 1186.
(10) Chung, D. D. L. *Carbon* **2001**, *39*, 279.
(11) Yang, Y. L.; Gupta, M. C.; Dudley, K. L.; Lawrence, R. W. *Adv. Mater.* **2005**, *17*, 1999.

(12) Xiang, C. S.; Pan, Y. B.; Liu, X. J.; Sun, X. W.; Shi, X. M.; Guo, J. K. *Appl. Phys. Lett.* **2005**, *87*, 123103.
(13) Joo, J.; Epstein, A. J. *Appl. Phys. Lett.* **1994**, *65*, 2278.
(14) Luo, X.; Chung, D. D. L. *Carbon* **1996**, *34*, 1293.
(15) Luo, X. C.; Chung, D. D. L. *Composites, Part B* **1999**, *30*, 227.
(16) Yang, Y. L.; Gupta, M. C.; Dudley, K. L.; Lawrence, R. W. *Nano Lett.* **2005**, *5*, 2131.
(17) Yang, Y. L.; Gupta, M. C.; Dudley, K. L.; Lawrence, R. W. *J. Nanosci. Nanotechnol.* **2005**, *5*, 927.
(18) Kim, H. M.; Kim, K.; Lee, C. Y.; Joo, J.; Cho, S. J.; Yoon, H. S.; Pejakovic, D. A.; Yoo, J. W.; Epstein, A. J. *Appl. Phys. Lett.* **2004**, *84*, 589.
(19) Che, R. C.; Peng, L. M.; Duan, X. F.; Chen, Q.; Liang, X. L. *Adv. Mater.* **2004**, *16*, 401.
(20) Grimes, C. A.; Mungle, C.; Kouzoudis, D.; Fang, S.; Eklund, P. C. *Chem. Phys. Lett.* **2000**, *319*, 460.
(21) Kim, B. S.; Lee, J. J.; Yu, I. B. *J. Appl. Phys.* **2003**, *94*, 6724.
(22) Barraza, H. J.; Pompeo, F.; O'Rear, E. A.; Resasco, D. E. *Nano Lett.* **2002**, *2*, 797.
(23) Watts, P. C. P.; Hsu, W. K.; Barnes, A.; Chambers, B. *Adv. Mater.* **2003**, *15*, 600.
(24) Javey, A.; Guo, J.; Wang, Q.; Lundstrom, M.; Dai, H. J. *Nature* **2003**, *424*, 654.
(25) Martel, R.; Schmidt, T.; Shea, H. R.; Hertel, T.; Avouris, P. *Appl. Phys. Lett.* **1998**, *73*, 2447.
(26) Lv, X.; Du, F.; Ma, Y.; Wu, Q.; Chen, Y. *Carbon* **2005**, *43*, 2020.
(27) Du, F.; Ma, Y.; Lv, X.; Huang, Y.; Li, F.; Chen, Y. *Carbon* **2006**, *44*, 1327.
(28) Garboczi, E. J.; Snyder, K. A.; Douglas, J. F.; Thorpe, M. F. *Phys. Rev. E* **1995**, *52*, 819.
(29) Obukhov, S. P. *Phys. Rev. Lett.* **1995**, *74*, 4472.
(30) Tellakula, R. A.; Varadan, V. K.; Shami, T. C.; Mathur, G. N. *Smart Mater. Struct.* **2004**, *13*, 1040.
(31) Wu, J. H.; Kong, L. B. *Appl. Phys. Lett.* **2004**, *84*, 4956.
(32) Dalmas, F.; Chazeau, L.; Gauthier, C.; Masenelli-Varlot, K.; Dendievel, R.; Cavaille, J. Y.; Forro, L. *J. Polym. Sci., Part B: Polym. Phys.* **2005**, *43*, 1186.
(33) Long, Y. Z.; Chen, Z. J.; Zhang, X. T.; Zhang, J.; Liu, Z. F. *Appl. Phys. Lett.* **2004**, *85*, 1796.
(34) Watts, P. C. P.; Ponnampalam, D. R.; Hsu, W. K.; Barnes, A.; Chambers, B. *Chem. Phys. Lett.* **2003**, *378*, 609.
(35) Sen, R.; Zhao, B.; Perea, D.; Itkis, M. E.; Hu, H.; Love, J.; Bekyarova, E.; Haddon, R. C. *Nano Lett.* **2004**, *4*, 459.
(36) Chatterjee, T.; Yurekli, K.; Hadjiev, V. G.; Krishnamoorti, R. *Adv. Funct. Mater.* **2005**, *15*, 1832.
(37) Grunlan, J. C.; Mehrabi, A. R.; Bannon, M. V.; Bahr, J. L. *Adv. Mater.* **2004**, *16*, 150.
(38) Ramasubramaniam, R.; Chen, J.; Liu, H. Y. *Appl. Phys. Lett.* **2003**, *83*, 2928.

NL0602589